

Controlling the Microadsorption Structure of Porphyrin Dye Assembly on Clay Surfaces Using the “Size-Matching Rule” for Constructing an Efficient Energy Transfer System

Yohei Ishida,^{†,‡} Dai Masui,[†] Hiroshi Tachibana,[†] Haruo Inoue,[†] Tetsuya Shimada,[†] and Shinsuke Takagi^{*,†,§}

[†]Department of Applied Chemistry, Graduate Course of Urban Environmental Sciences, Tokyo Metropolitan University, Minami-ohsawa 1-1, Hachiohji, Tokyo 192-0397 Japan

[‡]Japan Society for the Promotion of Science (DC1), Ichibancho, Chiyoda-ku, Tokyo 102-8471, Japan.

[§]PRESTO (Precursory Research for Embryonic Science and Technology), Japan Science and Technology Agency, 4-1-8 Honcho Kawaguchi, Saitama, Japan

ABSTRACT: The microadsorption structure of two kinds of porphyrin molecules on an anionic clay surface was investigated by photochemical energy transfer reaction. Three procedures were examined for the preparation of the clay/porphyrin complexes: (i) coadsorption (CA) method, (ii) sequential adsorption (SA) method, and (iii) independent adsorption (IA) method as described in the text. Efficient and moderate energy transfer reactions were observed in the CA and SA complexes, respectively. On the contrary, the energy transfer did not occur in the IA complex. These results indicate that the microadsorption structure of the two kinds of porphyrin on the clay mineral surface resulting from the sample preparation methods, affects the energy transfer efficiency. As a result, it was revealed that (i) the adsorbed porphyrins can move on the clay mineral surface but cannot move from one clay surface to another clay sheet, and (ii) the integration structure of two kinds of porphyrin is more stable than the segregation structure in the present system. This unusual structure originated from an extremely strong electrostatic interaction between the porphyrin and the clay mineral as a result of a “size-matching rule”. These unique strongly fixed dye assemblies on the clay mineral surface, in which the aggregation and segregation of dyes are suppressed, is very promising and attractive for constructing efficient photochemical reaction systems.

KEYWORDS: porphyrin, size-matching rule, clay mineral, saponite, molecular alignment, light-harvesting system, energy transfer



INTRODUCTION

The light-harvesting assemblies and reaction centers of natural photosynthetic systems contain remarkable molecular arrangements that participate in highly efficient energy and electron transfer reactions.¹ This recognition has stimulated intensive studies in the field of artificial light-harvesting systems. Among the various approaches to artificial light-harvesting systems,^{2–23} inorganic/organic hybrid systems have been focal, especially from the viewpoint of developing novel methodologies for building organized systems with inorganic nanosheets as platforms.^{14–23} Saponite, which is one of the typical clay minerals, are an attractive group of materials^{24–32} that are characterized by (1) nanostructured flat sheets, (2) negatively charged surfaces, (3) exfoliation or stack ability of individual nanosheets depending on the surrounding conditions, and (4) optical transparency in the visible region in the exfoliated state when the particle size is small (c.a. $<0.2 \mu\text{m}$). The focus of our investigations has been on using clay minerals as novel host materials for the construction of an artificial light-harvesting system.

We have developed a novel technique for control of the arrangement of dye assemblies on clay mineral surfaces.^{33–36} Moreover, we have successfully prepared unique clay/porphyrin complexes in which the porphyrin molecules are

adsorbed onto the clay mineral surface without aggregation, even at high dye loadings.^{33–36} The formation of these unique hybrids was rationalized by a size-matching of distance between the charged sites in the porphyrin molecule and the distance between anionic sites on the clay mineral surface. We termed this effect the “size-matching rule”.^{33–35} The energy transfer between the adsorbed porphyrins and subsequent electron transfer to acceptor molecules in solution have been observed.^{18,19}

Generally, dye molecules tend to aggregate³⁷ (Figure 1a), segregate³⁸ (Figure 1b) and cluster (Figure 1c) on the clay mineral surface or in the interlayer space between clay sheets. Given that (i) aggregation such as H-aggregated structure significantly decreases the excited-state lifetimes of dyes, and (ii) segregation causes a decrease in the reaction efficiency because of the resulting decrease in the probability that molecules will be adjacent, the efficiency of a photochemical reaction should be very low under normal conditions.^{38–41} The clustering structure (Figure 1c) is caused by the hydrophobic interaction in aqueous solution.¹⁹

Received: October 24, 2011

Accepted: January 4, 2012

Published: January 4, 2012

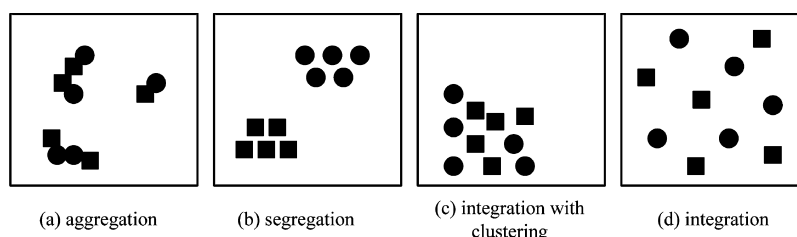


Figure 1. Schematic representations of adsorption structures: (a) aggregation, (b) segregation, (c) integration with clustering, and (d) integration of two kinds of molecule on the clay mineral surface. In the aggregated structure (a), there is an interaction between transition dipole moments of molecules.

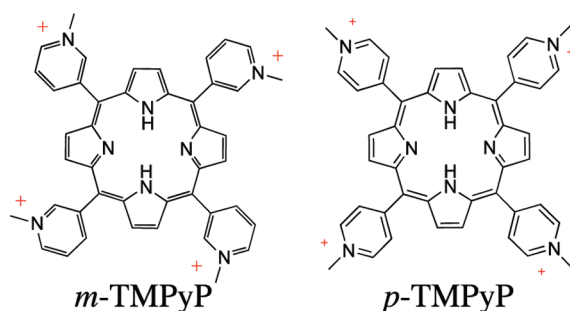
In our system, the aggregation (Figure 1a) is completely suppressed by the strong interaction between the porphyrin and the clay mineral as a result of the “size-matching rule”. However, suppression of segregation (Figure 1b) in this system has not been discussed in detail.

In this paper, the effect of sample preparation methods on the energy transfer efficiency was investigated. In addition, the microadsorption structures of two kinds of porphyrin on the clay mineral surface, i.e., segregation (Figure 1b) and integration (Figure 1d) structures, are also discussed.

EXPERIMENTAL SECTION

Materials. The saponite clay mineral used in this experiment was synthesized by hydrothermal synthesis according to a previous paper.³⁶ Na_2SiO_3 solution (15.45 g) was diluted by the addition of 80 mL of deionized water, and then 5 mL of nitric acid solution was added to the diluted Na_2SiO_3 solution (solution A). $\text{MgCl}_2 \cdot 6\text{H}_2\text{O}$ (12.44 g) and $\text{AlCl}_3 \cdot 6\text{H}_2\text{O}$ (1.97 g) were dissolved in 20 mL of deionized water (solution B). Solutions A and B were combined and the obtained solution was added to 52 mL of ammonia solution under continuous stirring within approximately 3 min. Formed precipitate was filtered with glass filter (type 25G3) and washed with deionized water repeatedly. Aqueous solution of NaOH (1.55 M, 5 mL) was added to the collected residue. The obtained slurry was kept under 573 K and 8.5 MPa in the autoclave for about 6 h. The saponite component was collected from the reaction mixture by 3 days hydraulic elutriation and a centrifugal separation of the supernatant (18000 rpm, 5 h). The synthetic saponite was analyzed with XRD, XRF, ^{27}Al -NMR, FT-IR, and TG/DTA. The cation-exchange capacity (CEC) was 1.00 mequiv. g^{-1} and the average interchange distance on the clay mineral surface was calculated to be 1.19 nm on the basis of a hexagonal array. Tetrakis(1-methylpyridinium-3-yl) porphyrin (*m*-TMPyP, purchased from Frontier Scientific) and tetrakis(1-methylpyridinium-4-yl) porphyrin (*p*-TMPyP, purchased from Aldrich) were used as the energy donor and energy acceptor, respectively (Chart 1). The counterions were exchanged for chloride using an ion-exchange column (Organo Amberlite IRA400JCL). The purity of the porphyrins

Chart 1. Structures of Tetrakis(1-methylpyridinium-3-yl) Porphyrin (*m*-TMPyP) and Tetrakis(1-methylpyridinium-4-yl) Porphyrin (*p*-TMPyP)



was checked by ^1H NMR. Water was deionized with an ORGANO BB-5A system (PF filter $\times 2$ + G-10 column).

Analysis. Absorption spectra were measured with a Shimadzu UV-3150 spectrophotometers. Fluorescence spectra were measured with a Jasco FP-6500 spectrofluorometer. In the absorption and fluorescence measurements, a quartz cell was used for the aqueous clay/porphyrin solutions. The fluorescence spectra of the clay/porphyrin complexes in aqueous solution were measured upon excitation at 430 nm, which is the wavelength of the maximum absorption (λ_{max}) of the *m*-TMPyP/clay complex. TG/DTA measurements were carried out with a Shimadzu DTG-60H analyzer to determine the water content of the porphyrins and clay.

Preparation Methods for the Clay/Porphyrin Complexes.

Three types of clay/porphyrin complex were prepared as shown in Figure 2: (i) aqueous solutions of *m*-TMPyP and *p*-TMPyP were

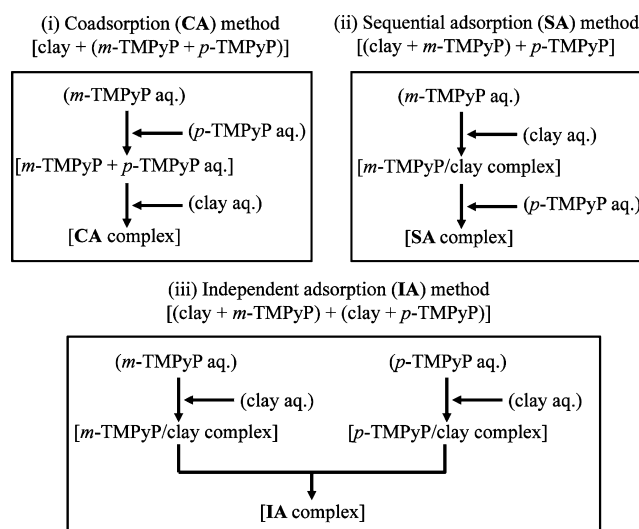


Figure 2. Schematic images of sample preparation methods.

mixed and the solution obtained was mixed with an aqueous clay solution [coadsorption (CA) method (clay + (*m*-TMPyP + *p*-TMPyP))], (ii) an aqueous solution of *m*-TMPyP was mixed with an aqueous clay solution, and the obtained solution was then mixed with an aqueous solution of *p*-TMPyP [sequential adsorption (SA) method ((clay + *m*-TMPyP) + *p*-TMPyP)] and (iii) each clay/porphyrin complex (*m*-TMPyP/clay and *p*-TMPyP/clay) was prepared and then the individual complexes were combined [independent adsorption (IA) method ((clay + *m*-TMPyP) + (clay + *p*-TMPyP))]. The concentrations of *m*-TMPyP and *p*-TMPyP were set to 5.0×10^{-8} M. The concentration of clay mineral was set to 0.4–800 mg L^{-1} . The porphyrin loading level vs cation-exchange capacity (CEC) of the clay was adjusted from 0.05 to 90% by changing the concentration of the clay mineral. The fluorescence spectra were measured within 5 min of preparing the clay/porphyrin complexes.

Under these conditions, the clay sheets exist as individually exfoliated sheets and the obtained solution was substantially

transparent. No porphyrin was detected in the supernatant liquid obtained by centrifugation of a clay/porphyrin mixture (12 000 rpm, 60 min); this indicated that all of the porphyrin molecules were adsorbed onto the clay mineral surface.

RESULTS AND DISCUSSION

Absorption and Fluorescence Spectra of Clay/Porphyrin Complexes. The absorption and fluorescence spectra of *m*-TMPyP/clay and *p*-TMPyP/clay complexes were relatively well differentiated (Figure 3, inset). The absorption

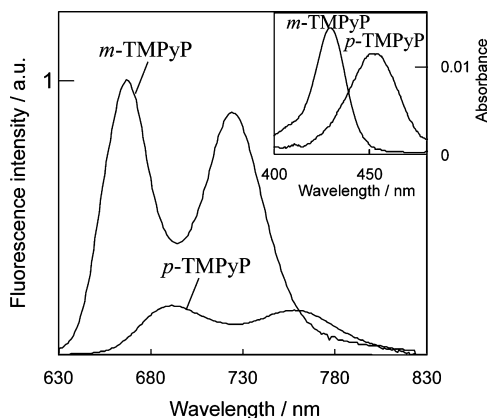


Figure 3. Fluorescence ($\lambda_{\text{ex}} = 430 \text{ nm}$) spectra of *m*-TMPyP/clay and *p*-TMPyP/clay complexes in aqueous solution ($[\text{clay}] = 4.0 \text{ mg L}^{-1}$, $[\text{m-TMPyP}] = [\text{p-TMPyP}] = 5.0 \times 10^{-8} \text{ M}$). Inset: the absorption spectra of *m*-TMPyP/clay and *p*-TMPyP/clay complexes in the region of the Soret band.

spectra of *m*-TMPyP/*p*-TMPyP/clay complexes were identical for the CA, SA, and IA complexes, within error. The absorption spectra of *m*-TMPyP/*p*-TMPyP/clay complexes corresponded perfectly to the sum of the individual absorption spectra of *m*-TMPyP/clay and *p*-TMPyP/clay complexes. Thus, it was found that porphyrin aggregation is completely suppressed and the porphyrin exists as a single molecule over the entire loading level range (0.05–90% vs CEC of the clay), even when the two porphyrins coexist on the clay mineral surface.

Energy Transfer Reaction between Adsorbed Porphyrins on the Clay Mineral Surface: The Effect of Sample Preparation Methods. The excited energy transfer from the excited singlet state of *m*-TMPyP to the ground state

of *p*-TMPyP on the clay mineral surface was examined at various loading levels of porphyrins for three sample preparation methods. The excitation wavelength was set at 430 nm for all experiments; this is the λ_{max} of *m*-TMPyP/clay complex. Under the present experimental condition, the concentration of porphyrin dyes is always kept constant to be $1.0 \times 10^{-7} \text{ M}$ and the loading level of adsorption is varied by controlling the concentration of clay, indicating that every sample adsorbed the same number of photons under the same absorbance. We can thus discuss the energy transfer by simply comparing the fluorescence intensity. The fluorescence spectral changes of CA, SA, and IA complexes in response to various loading levels of porphyrins are shown in Figure 4. In the case of the CA and SA complexes, the fluorescence intensity of the donor porphyrin (*m*-TMPyP) decreased and that of the acceptor porphyrin (*p*-TMPyP) increased as the dye loadings increased. In the case of the IA complex, the obtained fluorescence spectra corresponded identically to the sum of the identical fluorescence spectra of *m*-TMPyP/clay and *p*-TMPyP/clay complexes. This indicates that the energy transfer did not occur in the IA complex.

Because the absorption and fluorescence spectra are relatively well differentiated, the energy transfer efficiency can be quantitatively estimated by the analysis of the fluorescence spectra.^{19,20} The fluorescence spectra of *m*-TMPyP/*p*-TMPyP/clay complexes can be well simulated as a superposition of the respective fluorescence spectra of *m*-TMPyP/clay and *p*-TMPyP/clay complexes. The procedure for calculating the energy transfer efficiency (η_{ET}) and the quenching efficiency (ϕ_{q}) is described in the literature.^{19,20} The quenching would be induced by any photochemical reaction other than the expected energy transfer, such as an electron transfer reaction between porphyrins.

In Figure 5, the values obtained for η_{ET} are plotted against the loading levels of porphyrins for each sample prepared by the CA, SA, and IA methods, respectively.

The η_{ET} vs loading level plots in Figure 5 shows that high and moderate energy transfers were observed in CA and SA complexes, respectively. On the other hand, no energy transfer was observed in the IA complex. The quenching efficiency (ϕ_{q}) was zero for all samples, which indicates that the electron transfer reaction between porphyrins did not occur.

Given that the Förster-type energy transfer rate constant is inversely proportional to the sixth power of the intermolecular distance,⁴² it is reasonable that η_{ET} increased as a result of the

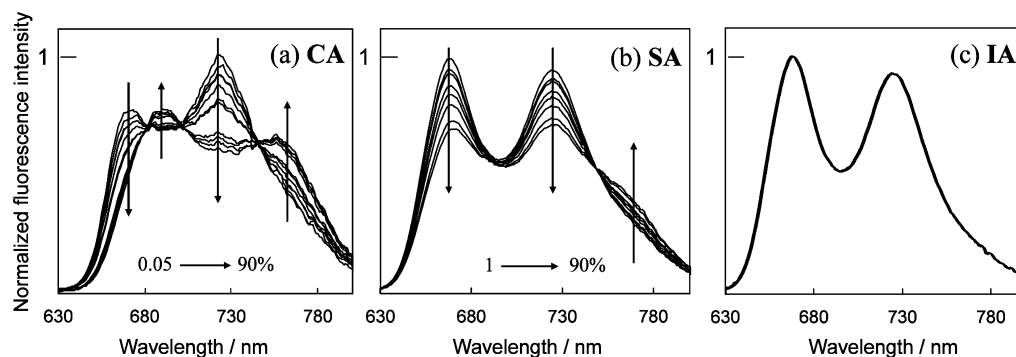


Figure 4. Fluorescence spectra of *m*-TMPyP/*p*-TMPyP/clay complexes prepared by (a) coadsorption (CA), (b) sequential adsorption (SA), and (c) independent adsorption (IA) methods in aqueous solution. The excitation wavelength was 430 nm. The dye loadings were set at 0.05–90% vs CEC of the clay ($[\text{m-TMPyP}] = [\text{p-TMPyP}] = 5.0 \times 10^{-8} \text{ M}$).

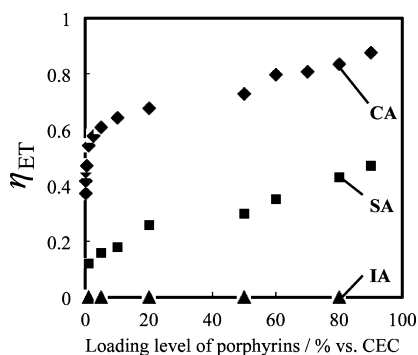


Figure 5. Obtained values of energy transfer efficiencies (η_{ET}) at various loading levels of porphyrins. The three types of preparation methods, coadsorption (CA (◆)), sequential adsorption (SA (■)), and independent adsorption (IA (▲)) methods, were examined. The dye loadings were set at 0.05–90% vs CEC of the clay in aqueous solution ($[m\text{-TMPyP}] = [p\text{-TMPyP}] = 5.0 \times 10^{-8}$ M).

decrease of intermolecular distance with increasing dye loadings in the CA and SA complexes, while the efficiency decreases due to the aggregation and/or the self-quenching of molecules in typical systems.¹⁷

The obtained efficiencies at low dye loadings were higher than that expected from the average intermolecular distance. In the case of 1% dye loading ($\eta_{ET} = 55\%$), the average intermolecular distance is calculated to be 24 nm on the basis of a hexagonal array, which is much larger to proceed an energy transfer. Thus, it is apparent that the actual intermolecular distance is much shorter than that in the complete random distribution and the cluster of porphyrin dyes forms, as described in a previous paper.¹⁹ The cluster means the gathering of dye without aggregation (Figure 1c).

The differences in the values obtained for η_{ET} in the CA, SA, and IA complexes can be explained on the basis of following considerations. Because an energy transfer occurs between two kinds of dye, the energy transfer rate constant is significantly affected by the number of acceptor molecules adjacent to a given donor. In this experiment, the total concentration of dyes in the three types of complex (CA, SA, and IA) was the same, thus, we focused on the detailed microadsorption structures of two kinds of porphyrin on the clay mineral surface. In other words, it was important to determine whether the adsorption structures of CA, SA, and IA complexes were segregated or integrated on the clay mineral surface (Figure 1b, c).

In the case of the CA complex [clay + ($m\text{-TMPyP}$ + $p\text{-TMPyP}$)], the two kinds of porphyrin were integrated on the clay mineral surface immediately after preparation (integration, Figure 6i), because the mixed solution of the two porphyrins was added to the clay solution, as described in a previous paper.²⁰ The integration structure offers a certain number of adjacent acceptors around each excited donor porphyrin, thus, the η_{ET} obtained was larger than those in the other two cases. The explanation of why η_{ET} did not reach the theoretical maximum of 100% can be rationalized by the small value of the spectral overlap integral (J) between the porphyrins.²⁰ The J value in this system is $3.9 \times 10^{-14} \text{ M}^{-1} \text{ cm}^{-1} \text{ cm}^4$ as described in the previous paper.²⁰ Because a small J value results in a small energy transfer rate constant,⁴² the energy transfer reaction competes with the excited-state lifetime of the donor.

In the case of the IA complex [(clay + $m\text{-TMPyP}$) + (clay + $p\text{-TMPyP}$)], the two porphyrins are expected to be segregated into the different clay sheets immediately after preparation

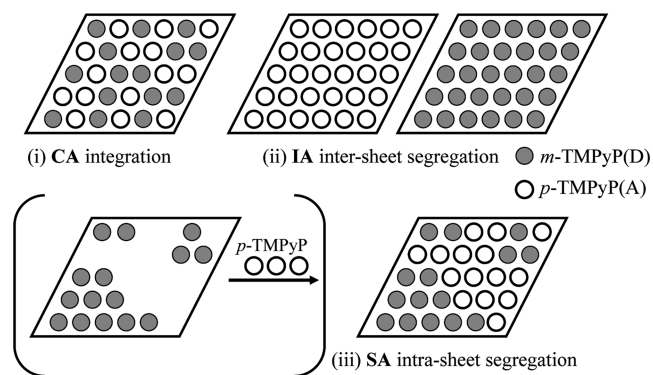


Figure 6. Possible idealized adsorption structures of two kinds of porphyrin on the clay mineral surface for the complexes prepared by (i) coadsorption (CA), (ii) independent adsorption (IA), and (iii) sequential adsorption (SA) methods.

(intersheet segregation, Figure 6ii) because each complex ($m\text{-TMPyP}/\text{clay}$ and $p\text{-TMPyP}$) was separately prepared and then the complexes were mixed. Thus, the energy transfer did not occur at all.

On the basis of these considerations, the adsorption structure of the SA complex [(clay + $m\text{-TMPyP}$) + $p\text{-TMPyP}$] is proposed to be an intermediate structure between integration and intersheet segregation.

Generally, organic compounds tend to cluster on a solid surface in aqueous solution as a result of hydrophobic interactions. In the procedure for preparing the SA complex [clay + $m\text{-TMPyP}$] + $p\text{-TMPyP}$, $m\text{-TMPyP}$, which is initially mixed with the clay, should cluster on the clay mineral surface, and $p\text{-TMPyP}$, which is then mixed in, will be adsorbed on the residual anionic sites of the clay mineral surface. Thus, the two porphyrins would be segregated from each other on the same clay surface (intrasheet segregation, Figure 6iii). Because the intrasheet segregation structure which separates the two kinds of porphyrin causes a decrease in the number of adjacent $p\text{-TMPyP}$ molecules in the vicinity of $m\text{-TMPyP}$, the η_{ET} obtained in the SA complex is less than that in the CA complex, for which there are more adjacent donor–acceptor sites.

On the basis of these results, it can be concluded that the method employed in the preparation of clay/porphyrin complexes affects the efficiency of the photochemical energy transfer reaction in terms of the probability of placement of adjacent dyes. It should be noted that dyes usually tend to adopt the intersheet and/or intrasheet segregation structure on the clay mineral surface, even when the coadsorption (CA) method is used for sample preparation.²⁸

Fluorescence Time Courses for the CA, SA, and IA Complexes. The fluorescence time courses for the three types of complex were measured in order to provide further details about the adsorption structures of the porphyrins on the clay mineral surface. The examined samples were the 80% loadings vs CEC of the clay, and the spectra were observed from 0 to 60 min after preparing the complexes.

The observed fluorescence spectra and the time courses of the η_{ET} values in the CA, SA and IA complexes are shown in Figure 7 and Figure 8, respectively. In the case of the SA complex, an obvious change in the fluorescence spectrum was observed (Figure 7b). In constant, no spectral changes were observed for the CA and IA complexes (Figure 7a, c). The result presented in Figure 7c obviously indicates that the adsorbed porphyrins

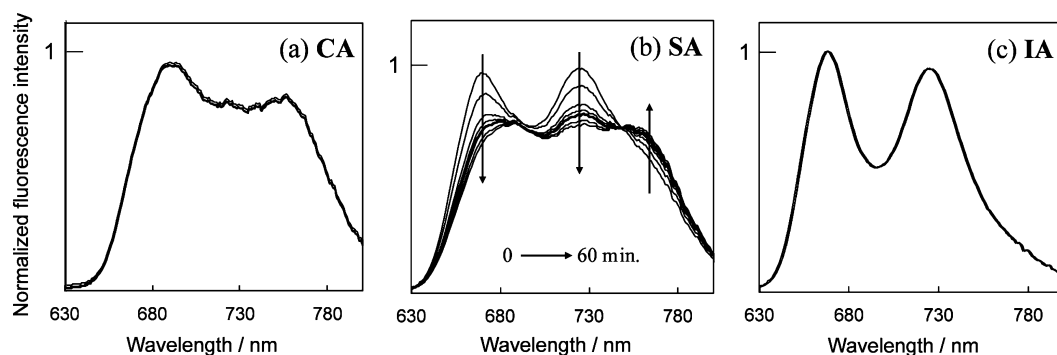


Figure 7. Time courses of fluorescence in (a) CA, (b) SA, and (c) IA complexes in aqueous solution. The dye loading was set at 80% vs CEC of the clay ($[m\text{-TMPyP}] = [p\text{-TMPyP}] = 5.0 \times 10^{-8} \text{ M}$). The spectra were observed at 0, 5, 10, 15, 20, 30, 40, 50, and 60 min after sample preparation. The excitation wavelength was 430 nm.

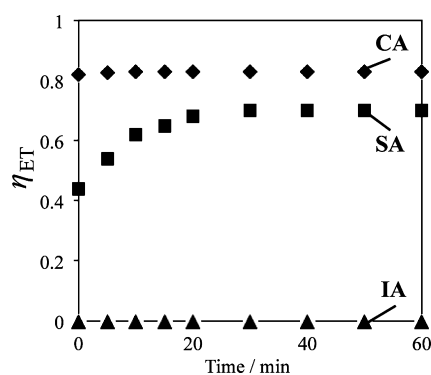


Figure 8. Time courses of the energy transfer efficiencies (η_{ET}). The three types of preparation method, i.e., coadsorption (CA (◆)), sequential adsorption (SA (■)), and independent adsorption (IA (▲)) were examined. The obtained values observed at 0, 5, 10, 15, 20, 30, 40, 50, and 60 min after sample preparation were plotted. $[m\text{-TMPyP}] = [p\text{-TMPyP}] = 5.0 \times 10^{-8} \text{ M}$. The dye loading was 80% vs CEC of the clay.

cannot move from one clay mineral surface to another clay mineral surface.

The obtained η_{ET} values for the SA complex increased from 43% to 71% with time, as shown in Figure 8 (■). It was postulated that this increase in η_{ET} with time was caused by a change in the adsorption structure of the two porphyrins on the clay mineral surface from intrasheet segregation to integration with time (Figure 9). The increase in the η_{ET} value became saturated at 71%, after 30 min. If the adsorbed porphyrins could move freely over the clay mineral surface and from one clay sheet to another, the saturated value of η_{ET} would be expected reach to 82%, which is the η_{ET} value of the CA complex under the same condition. Thus, the η_{ET} value

indicates that the adsorbed porphyrins can move on the clay mineral surface but cannot move from one clay sheet to another. The explanation of why the obtained value of η_{ET} (71%) did not attain the maximum value of 82%, is attributed to deviations in the adsorbed amounts of *m*-TMPyP and *p*-TMPyP on each clay mineral surface. Because the examined porphyrins are strongly adsorbed on the clay mineral surface as a result of the strong electrostatic interactions, the added porphyrins are immediately adsorbed on the neighboring clay mineral surface in aqueous solution. Thus, the numbers of molecules of adsorbed *m*-TMPyP and *p*-TMPyP are not the same at each clay sheet.

In the case of the CA complex, the observed fluorescence spectra and calculated values of η_{ET} did not vary with time. This clearly indicates that the integration structure of these two kinds of porphyrin on the clay mineral surface is more thermodynamically stable than the segregation structure.

In usual systems, because the host (clay mineral)–guest (molecule) interaction is not strong, the guest–guest interaction causes the intrasheet and/or intersheet segregation structure.^{28,38} While in our system, because the size-matching rule realizes the strong electrostatic interaction between the porphyrin and the clay, the guest–guest interaction can be almost negligible. Thus, the segregation was suppressed and the integration structure was realized. In addition, the similarity of dye structure might affect the realization of integration structure. Like this, it was found that the adsorption structure of molecules on the clay mineral surface such as segregation and integration can be regulated by controlling the host–guest and guest–guest interactions. This strongly fixed dye assembly without aggregation and segregation on the clay mineral surface is very promising and attractive for constructing an efficient photochemical reaction system.

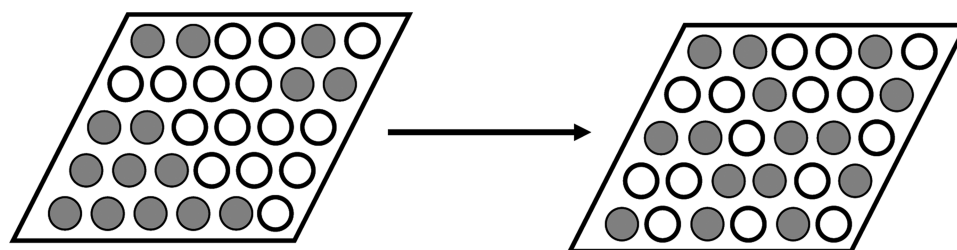


Figure 9. Possible idealized image of the adsorption structural changes with time for two kinds of porphyrin on the clay mineral surface in the SA complex.

CONCLUSION

The photochemical energy transfer reactions between cationic porphyrins adsorbed on the clay mineral surface were examined for clay/porphyrin complexes prepared by three sample preparation methods. The energy transfer efficiency was high and moderate for the CA and SA complexes, respectively. In the case of the IA complex, the energy transfer did not occur. These results indicate that the microadsorption structure of the two kinds of porphyrin on the clay mineral surface that results from the sample preparation method significantly affects the energy transfer efficiency. As a result, it was revealed that (i) the adsorbed porphyrins can move on the clay mineral surface but cannot move from the clay surface to another, and (ii) the integration structure of the two kinds of porphyrin is more thermodynamically stable than the segregation structure in the present system. These unique structures were achieved by the strong interaction between the porphyrin and the clay, as a result of the "size-matching rule". This strongly fixed dye assembly on the clay mineral surface in which the aggregation and segregation of dyes are suppressed, is very promising and attractive for constructing efficient photochemical reaction systems.

AUTHOR INFORMATION

Corresponding Author

*E-mail: takagi-shinsuke@tmu.ac.jp. Tel.: +81 42 677 2839. Fax: +81 42 677 2838.

ACKNOWLEDGMENTS

This work has been partly supported by a Grant-in-Aid for Precursory Research for Embryonic Science and Technology (PRESTO) from the Japan Science and Technology Agency (JST), and JSPS Research Fellow DC1 from the Japan Society for the Promotion of Science.

REFERENCES

- (1) McDermott, G.; Prince, S. M.; Freer, A. A.; Hawthornthwaite-Lawless, A. M.; Papiz, M. Z.; Cogdell, R. J.; Isaacs, N. W. *Nature* **1995**, *374*, 517–521.
- (2) Takahashi, R.; Kobuke, Y. *J. Am. Chem. Soc.* **2003**, *125*, 2372–2373.
- (3) Lopez, G. S.; Worringer, G.; Rodriguez, B.; Roman, S. E. *Phys. Chem. Chem. Phys.* **2010**, *12*, 2246–2253.
- (4) Novoderezhkin, V.; Grondelle, V. R. *Phys. Chem. Chem. Phys.* **2010**, *12*, 7352–7365.
- (5) Watkins, D. M.; Sweet, S. Y.; Klimash, J. W.; Turro, N. J.; Tomalia, D. A. *Langmuir* **1997**, *13*, 3136–3141.
- (6) Gilat, S. L.; Adronov, A.; Frechet, J. M. J. *Angew. Chem., Int. Ed.* **1999**, *38*, 1422–1427.
- (7) Chen, L.; Revel, S.; Morris, K.; Adams, J. D. *Chem. Commun.* **2010**, *46*, 4267–4269.
- (8) Hardin, E. B.; Sellinger, A.; Moehl, T.; Baker, H. R.; Moser, E. J.; Wang, P.; Zakeeruddin, M. S.; Gratzel, M.; McGehee, D. M. *J. Am. Chem. Soc.* **2011**, *133*, 10662–10667.
- (9) Choi, H. -S.; Aida, T.; Yamazaki, T.; Yamazaki, I. *Chem.—Eur. J.* **2002**, *8*, 2667–2678.
- (10) Okada, S.; Segawa, H. *J. Am. Chem. Soc.* **2003**, *125*, 2792–2796.
- (11) Yoo, H.; Yang, J.; Nakamura, Y.; Aratani, N.; Osuka, A.; Kim, D. *J. Am. Chem. Soc.* **2009**, *131*, 1488–1494.
- (12) Miyatake, T.; Tamiaki, H.; Holzwarth, A. R.; Schaffner, K. *Photochem. Photobiol.* **1999**, *69*, 448–456.
- (13) Choi, H.; Ku, B. S.; Keum, S. R.; Kang, S. O.; Ko, J. *Tetrahedron* **2005**, *61*, 3719–3723.
- (14) Thomas, K. J.; Sunoj, R. B.; Chandrasekhar, J.; Ramamurthy, V. *Langmuir* **2000**, *16*, 4912–4921.
- (15) Casey, J. P.; Bachilo, S. M.; Weisman, R. B. *J. Mater. Chem.* **2008**, *18*, 1510–1516.
- (16) Kaschak, D. M.; Lean, J. T.; Waraksa, C. C.; Saupe, G. B.; Usami, H.; Mallouk, T. E. *J. Am. Chem. Soc.* **1999**, *121*, 3435–3445.
- (17) Takagi, S.; Tryk, D. A.; Inoue, H. *J. Phys. Chem. B* **2002**, *106*, 5455–5460.
- (18) Takagi, S.; Eguchi, M.; Tryk, D. A.; Inoue, H. *Langmuir* **2006**, *22*, 1406–1408.
- (19) Takagi, S.; Eguchi, M.; Inoue, H. *Res. Chem. Intermed.* **2007**, *33*, 177–189.
- (20) Ishida, Y.; Shimada, T.; Masui, D.; Tachibana, H.; Inoue, H.; Takagi, S. *J. Am. Chem. Soc.* **2011**, *133*, 14280–14286.
- (21) Fujii, K.; Iyi, N.; Hashizume, H.; Shimomura, S.; Ando, T. *Chem. Mater.* **2009**, *21*, 1179–1181.
- (22) Kuroda, T.; Fujii, K.; Sakoda, K. *J. Phys. Chem. C* **2010**, *114*, 983–989.
- (23) Schanze, K.; Silverman, E. E.; Zhao, X. *J. Phys. Chem. B* **2005**, *109*, 18451–18459.
- (24) Ogawa, M.; Kuroda, K. *Chem. Rev.* **1995**, *95*, 399–438.
- (25) Lopez Arbeloa, F.; Martinez Martinez, V.; Arbeloa, T.; Lopez Arbeloa, I. *J. Photochem. Photobiol. C: Photochem. Rev.* **2007**, *8*, 85–108.
- (26) Ras, R.; Umemura, Y.; Johnston, C.; Yamagishi, A.; Schoonheydt, R. *Phys. Chem. Chem. Phys.* **2007**, *9*, 918–932.
- (27) Sato, H.; Hiroe, Y.; Tamura, K.; Yamagishi, A. *J. Phys. Chem. B* **2005**, *109*, 18935–18941.
- (28) Letaief, S.; Detellier, C. *Langmuir* **2009**, *25*, 10975–10979.
- (29) Takagi, K.; Shichi, T. *J. Photochem. Photobiol. C: Photochem. Rev.* **2000**, *1*, 113–130.
- (30) Takagi, S.; Eguchi, M.; Tryk, D. A.; Inoue, H. *J. Photochem. Photobiol. C: Photochem. Rev.* **2006**, *7*, 104–126.
- (31) Thomas, J. K. *Chem. Rev.* **1993**, *93*, 301–320.
- (32) Bujdak, J.; Komadel, P. *J. Phys. Chem. B* **1997**, *101*, 9065–9068.
- (33) Takagi, S.; Shimada, T.; Yui, T.; Inoue, H. *Chem. Lett.* **2001**, *30*, 128–129.
- (34) Takagi, S.; Shimada, T.; Eguchi, M.; Yui, T.; Yoshida, H.; Tryk, D. A.; Inoue, H. *Langmuir* **2002**, *18*, 2265–2272.
- (35) Eguchi, M.; Takagi, S.; Tachibana, H.; Inoue, H. *J. Phys. Chem. Solids* **2004**, *65*, 403–407.
- (36) Egawa, T.; Watanabe, H.; Fujimura, T.; Ishida, Y.; Yamato, M.; Masui, D.; Shimada, T.; Tachibana, H.; Inoue, H.; Takagi, S. *Langmuir* **2011**, *27*, 10722–10729.
- (37) Bujdak, J.; Iyi, N.; Fujita, T. *Clay minerals* **2002**, *37*, 121–133.
- (38) Pushpito, G. K.; Bard, A. *J. Phys. Chem.* **1984**, *88*, 5519–5526.
- (39) Viaene, K.; Caigui, J.; Schoonheydt, R. A.; De Schryver, F. C. *Langmuir* **1987**, *3*, 107–111.
- (40) Madhavan, D.; Pitchumani, K. *Tetrahedron* **2002**, *58*, 9041–9044.
- (41) Menager, M.; Siampiringue, M.; Sarakha, M. *J. Photochem. Photobiol. A: Chemistry* **2009**, *208*, 159–163.
- (42) Forster, Th. Z. *Disc. Faraday Soc.* **1959**, *27*, 7–17.